

Biogeneration of chromophoric dissolved organic matter by bacteria and krill in the Southern Ocean

Eva Ortega-Retuerta,^a Thomas K. Frazer,^b Carlos M. Duarte,^c Sergio Ruiz-Halpern,^c Antonio Tovar-Sánchez,^c Jesús M. Arrieta,^c and Isabel Reche^{a,d,*}

^aDepartamento de Ecología, Facultad de Ciencias, Universidad de Granada, Granada, Spain

^bSchool of Forest Resources and Conservation, University of Florida, Gainesville, Florida

^cInstituto Mediterráneo de Estudios Avanzados (CSIC-UIB), Esporles, Illes Balears, Spain

^dInstituto del Agua, Universidad de Granada, Granada, Spain

Abstract

Chromophoric dissolved organic matter (CDOM), the optically active fraction of dissolved organic matter, is primarily generated by pelagic organisms in the open ocean. In this study, we experimentally determined the quantity and spectral quality of CDOM generated by bacterioplankton using two different substrates (with and without photoproducts) and by Antarctic krill *Euphausia superba* and evaluated their potential contributions to CDOM dynamics in the peninsular region of the Southern Ocean. CDOM was generated by bacteria in all experiments, and the presence of photoproducts influenced both the quantity and the spectral quality of the resultant CDOM. We confirmed a direct link between bacterial production and CDOM generation, which yielded in situ CDOM duplication times from 31 to 33 d. Antarctic krill as a direct source of CDOM was also confirmed experimentally. We estimated that CDOM generation by krill would lead to CDOM duplication times from 0.48 to 0.80 d within krill swarms. Our findings highlight the potential significance of bacteria and Antarctic krill swarms in the generation of CDOM and underscore the dynamic nature of CDOM in this area.

Chromophoric dissolved organic matter (CDOM) in oceanic waters comprises a broad suite of optically active compounds (Nelson and Siegel 2002; Coble 2007), and these compounds play important roles in the cycling of carbon and other elements as they mediate photochemical reactions (Mopper et al. 1991). In addition, CDOM represents a significant component of ocean optical signals for satellite-based measurements of ocean color and can interfere in global and regional estimates of primary production (Siegel et al. 2005). It is well established that photochemical processes that result in the transformation of CDOM modify its bioreactivity (Moran and Zepp 1997), and photobleaching represents the major pathway by which CDOM is lost in open ocean waters (Mopper et al. 1991; Nelson and Siegel 2002). Light-mediated processes affecting the dissolved organic matter (DOM) pool, however, can result also in the generation of CDOM (Kieber et al. 1997), and recent research suggests that in situ biological generation of CDOM is likely to be an important source of optically active compounds (Nelson et al. 2004; Steinberg et al. 2004). There are few studies, however, that have quantified the rates of biologically generated CDOM. Although phytoplankton are, by far, the dominant sources of organic carbon in the open ocean, the generation of CDOM appears to occur indirectly as a consequence of bacterial processing of algal exudates (Nelson et al. 1998; Rochelle-Newall and Fisher 2002) or through photoalteration of DOM released by algae (Kieber et al. 1997; Reche et al. 2001). CDOM may also be generated directly through extracellular release by prokaryotes (Nelson et al. 2004;

Steinberg et al. 2004) and excretion by zooplankton (Steinberg et al. 2004; Urban-Rich et al. 2006).

Bacterioplankton can regulate DOM composition through the selective consumption of labile compounds and subsequent release of humic-like (chromophoric) substances (Tranvik 1993; Kawasaki and Benner 2006) that are largely biorefractory in nature. The production of this material can comprise a significant proportion of the total DOM pool, extending the residence time of organic carbon in the water column, with obvious consequences for global carbon cycling (Ogawa et al. 2001). CDOM generation by bacterial DOM processing appears to be dependent on several factors, such as substrate quality, previous photochemical transformations, and/or nitrogen availability (Kramer and Herndl 2004; Nelson et al. 2004; Biers et al. 2007). However, the persistence and optical properties of bacterially generated CDOM appears to vary considerably, and the role of bacteria in CDOM dynamics is poorly understood. Similarly, although heterotrophic organisms such as zooplankton or protozoans also generate CDOM (Steinberg et al. 2004; Urban-Rich et al. 2006), published data on CDOM generation by organisms within the order Euphausiacea in seawater are scarce and not generally species specific.

In the Southern Ocean, several conditions converge that facilitate a quantitative assessment of the contribution of bacterial and krill-generated CDOM and promote a better understanding of CDOM dynamics in oceanic systems. First, the Southern Ocean is subject to extreme solar radiation in the austral summer. During this time, photochemical reactions can be expected to be important. Second, CDOM in high latitudes, and particularly in waters around the Antarctic Peninsula, is abundant, and, in

* Corresponding author: ireche@ugr.es

Table 1. Geographical location, depth, temperature (Temp), salinity (Sal), dissolved organic carbon (DOC), total nitrogen concentration (Total N), chlorophyll *a* (Chl *a*), and bacterial abundance (BA) at the locations and depths selected for the bacterial regrowth cultures, sunlight dose at 320 nm received in the photoproducts (photo) treatments, and absorption coefficient at 325 nm and 443 nm at the initial time of each treatment (t_0).

Location		Depth (m)	Temp (°C)	Sal (‰)	DOC ($\mu\text{mol L}^{-1}$)	Total N ($\mu\text{mol L}^{-1}$)	Chl <i>a</i> ($\mu\text{g L}^{-1}$)	BA ($\times 10^5$ cells mL^{-1})	Pre-exposure (kJ m^{-2})	Treatment	$a_{325} t_0$ (m^{-1})	$a_{443} t_0$ (m^{-1})
Deception Island	62°57.09' S, 60°23.16' W	0	2.11	33.9	69.0	12.2	5.1	7.9	+ 13.89	no photo	0.16	0.63
										photo	0.06	0.46
		150	0.17	33.9	50.1	33.6	0.4	na	+ 13.89	no photo	0.74	2.25
Livingston Island	62°29.34' S, 60°23.16' W	0	1.15	33.4	75.3	14.2	0.7	4.3	+ 7.51	no photo	0.33	1.12
										photo	0.24	0.78
		50	1.04	33.9	70.5	31.9	0.6	3.8	+ 7.51	no photo	0.23	0.68
									photo	0.38	1.13	
										photo	0.40	1.22

* na: not analyzed.

fact, accounts for up to 70% of the total non-water light absorption at 443 nm (Siegel et al. 2002). Finally, krill, which plays a key role controlling primary production and recycling processes in the Southern Ocean (Nicol 2006; Tovar-Sánchez et al. 2007), is abundant (Brierley and Watkins 2000; Nicol 2006).

In this study, we have determined experimentally the quantity and optical quality of CDOM generated by bacterioplankton using two different substrates (with and without photoproducts) and by Antarctic krill *Euphausia superba*. In addition, we have assessed the potential contribution of these agents to CDOM dynamics in the peninsular region of the Southern Ocean.

Methods

Bacterial CDOM generation experiments—To quantify CDOM generation by bacteria, a total of eight bacterial regrowth cultures were carried out under different conditions of CDOM and nutrient availability (Table 1). The experiments were carried out during January and February 2004, at the Spanish Base Juan Carlos I (Livingston Island, South Shetland Islands). Water for the experiments was collected from two different sites—Port Foster, Deception Island, and South Bay, Livingston Island—and was initially filtered through precombusted (3 h, $>450^\circ\text{C}$) Whatman GF/F filters (nominal pore size 0.5–0.7 μm) to remove phytoplankton and most heterotrophic consumers. Between 85% and 88% of bacterial cells were removed as a consequence of the filtering process. At each site, water from the surface (ca. 5 m) and below the euphotic layer (150-m and 50-m depth, respectively) was collected to set up two different treatments (surface and below euphotic zone) using a Niskin bottle with a conductivity–temperature–depth (CTD) attached. Because solar radiation can affect transformations in the structural conformation of dissolved organic matter and modify its bioreactivity (Moran and Zepp 1997), we also assessed the potential changes in bacterial CDOM generation associated with the presence of photoproducts by including a treatment with photoproducts for each location and depth. To do so,

GF/F-filtered water for the photoproducts treatments was placed in quartz bottles at ambient seawater temperature and under natural sunlight for 27–31 h before setting up all the regrowth cultures, corresponding to a total dose of ultraviolet (UV) at 320 nm equal to 7.51 kJ m^{-2} for the experiments performed with waters near Livingston Island. Incident UV was measured with a PUV 2500 Biospherical Instruments meter. Comparable light data were not available for experiments involving water from Deception Island, so we obtained data from the National Science Foundation UV Monitoring Network, operated by Biospherical Instruments under a contract with the U.S. National Science Foundation's Office of Polar Programs via Raytheon Polar Services Company. We estimated a cumulative dose at 320 nm over the exposure time of 13.89 kJ m^{-2} nm. Triplicate 250-mL flasks were filled for each combination of site, depth, and presence (i.e., pre-exposed to incident solar radiation) vs. absence of photoproducts. All treatments were subsequently inoculated (10% of total volume) with nonexposed water to avoid the use of bacteria with potential UV damage. All experiments were run for 97–122 h, and were incubated at ambient temperature (2–5°C) in the dark. Subsamples for bacterial abundance (BA) and bacterial production (BP) were taken daily; subsamples for CDOM characterization were taken at the beginning and at the end of each experiment.

Krill CDOM biogeneration experiments—To quantify and characterize CDOM released by Antarctic krill, *E. superba*, two types of experiments according to the incubation time were performed: daily experiments (incubation time from 12 to 24 h) and hourly experiments (short-term incubations of 4 h). For daily experiments, we performed 15 simple incubations in four sets. Adult krill were collected west of Anvers Island during January 2004 and maintained in large-volume, flow-through aquaria at Palmer Station prior to transport and experimentation at the Antarctic Spanish base Juan Carlos I. For each incubation, individual krill were placed in 1-liter glass jars prefilled with 0.7 liters of 0.2- μm -filtered seawater to minimize bacterial influence. Replicate controls with 0.2-

μm -filtered seawater and without krill additions were incubated in parallel. Incubations were carried out for 12 to 24 h at ambient light and temperature conditions. Samples for CDOM characterization were taken at the beginning and end of each experiment. To assess the potential growth of bacteria attached to krill or non-excluded by 0.2- μm filtration during the incubations, we set up another different experiment subject to the same conditions, and took samples for BA and BP at the beginning and after 24 h.

Because krill empty their gut contents in a short period of time (i.e., a few hours), we also quantified the release of CDOM by krill (*E. superba*) in short periods (4 h) setting up five additional experiments (hourly experiments). Hourly experiments (Nos. 16–20) were performed during the ATOS 2009 cruise on board the RV *Hesperides* in the Bellinghousen and Weddell Seas, along the Antarctic Peninsula sector of the Southern Ocean. Krill were detected using a Simrad TM EK60 multifrequency echosounder, collected within the upper 100 m at five stations (12 February, 65°17.56'S, 067°19.58'W; 13 February, 67°26.35'S, 70°54.11'W; 16 February, 68°32.35'S, 72°20.75'W; 23 February, 63°02.65'S, 57°32.20'W; and 25 February, 64°56.17'S, 55°47.84'W) using an Isaacs-Kidd-Mid-Water-Trawl net, with a 1-cm mesh size. For each incubation, four randomly selected similarly sized krill individuals were placed in 2-liter cleaned (acid-washed) low-density polyethylene bottles prefilled with 2 liters of 0.2- μm -filtered surface seawater to minimize bacterial influence. Replicate controls with 0.2- μm -filtered seawater and without krill additions were incubated in parallel. Incubations were carried out in the dark in an incubation chamber set at the surface seawater temperature $\pm 1^\circ\text{C}$ for 4 h. Samples for CDOM characterization and BA and BP were taken at the beginning and end of each experiment.

Chemical and biological analyses—Water for CDOM optical characterization was filtered through precombusted Whatman GF/F filters and stored in polypropylene flasks at 4°C in the dark prior to analysis (within a few hours). In each case, the absorbance spectrum for the resultant filtrate was measured with a Shimadzu UV-2401 PC spectrophotometer using 10-cm quartz cuvettes. Absorbance scans from 250 to 700 nm were performed, a spectrum of MilliQ water filtered by GF/F and stored in parallel to the samples was subtracted as a baseline, and internal backscattering was corrected by subtracting the absorbance at 700 nm (Bricaud et al. 1981). Two selected wavelengths (325 and 443 nm) were expressed as Napierian absorption coefficients (a_{325} and a_{443}) in m^{-1} using the following equation:

$$a_{325,443} = \frac{2.303 A_{325,443}}{l} \quad (1)$$

where l is the optical pathlength in meters and $A_{325,443}$ is the spectrophotometric absorbance at 325 and 443 nm, respectively. We selected 325 nm as a reference wavelength within the UVA spectrum (Nelson and Siegel 2002) and 443 nm because it is the reference wavelength for satellite CDOM determinations. The spectral slopes between 275 and 295 nm ($S_{275-295}$) and between 350 and 400 nm were

calculated by a standard linear regression of the ln-transformed absorption data and the ratio (S_R) of these two slopes was also calculated as a good proxy for DOM molecular weight (Helms et al. 2008).

Samples for dissolved organic carbon (DOC) analyses were collected after filtration through precombusted Whatman GF/F filters into precombusted 10-mL glass ampoules, acidified with phosphoric acid (final pH <2), sealed, and stored at 4°C prior to analysis. DOC was measured by high-temperature catalytic oxidation on a Shimadzu TOC-5000A analyzer. Standards of 44–45 $\mu\text{mol C L}^{-1}$ and 2 $\mu\text{mol C L}^{-1}$, provided by D. A. Hansell and Wenhao Chen (Univ. of Miami) (unpubl.) were used to assess the accuracy of the measurements.

BA was measured by epifluorescence microscopy (Porter and Feig 1980). Water subsamples of 4–10 mL were filtered onto 0.2- μm polycarbonate filters and stained with 4,6-diamidino-2 phenylindole (DAPI) to a final concentration of 1 $\mu\text{g mL}^{-1}$. At least 350 cells in 15 random fields were counted for each sample.

BP was estimated as the rate of ^3H -leucine-protein synthesis using the microcentrifugation technique proposed by Smith and Azam (1992). Briefly, 5 μL of L-[4,5- ^3H] leucine was added to 1.5-mL samples, yielding a final concentration of 56 nmol L^{-1} , and incubated for 3–4 h at ambient temperature. We used a conversion factor from leucine (leu) to carbon incorporation of 1.5 kg C mol leu^{-1} , which represents a standard assuming no isotope dilution (Simon and Azam 1989). Chlorophyll *a* (Chl *a*) concentration was determined fluorometrically (Parsons et al. 1984).

Determination of biogeneration rates—We calculated daily CDOM increases (Δa_λ , $\text{m}^{-1} \text{d}^{-1}$) in all bacterial and krill experiments as follows:

$$\Delta a_\lambda = \frac{a_{\lambda f} - a_{\lambda 0}}{t} \quad (2)$$

where λ is the reference wavelength (325 or 443 nm), a_λ is the absorption coefficient (m^{-1}), f is the final time, 0 is the initial time, and t is the incubation time in days.

To compare these CDOM increases among the different treatments and experiments, we calculated the percentage of Δa_λ (d^{-1}) using the following expression:

$$\% \Delta a_\lambda = \frac{\Delta a_\lambda}{a_{\lambda 0}} \times 100 \quad (3)$$

where λ is the reference wavelength (325 or 443 nm), Δa_λ is the daily CDOM increase ($\text{m}^{-1} \text{d}^{-1}$), a_λ is the absorption coefficient (m^{-1}), and 0 is the initial time.

We determined experimental bacterial CDOM generation rates ($\text{m}^{-1} \text{d}^{-1}$ per BA, or BP units) using linear regressions to relate $\Delta a_{325,443}$ to average BA or BP of each regrowth treatment. Average BA and BP in the regrowth cultures were determined by averaging all measurements weighted by the length of the interval between successive sampling. We forced the regression line to pass through the origin to avoid the effects of a high-CDOM background. To extrapolate these experimental rates to field CDOM bacterial generation rates ($\text{m}^{-1} \text{d}^{-1}$), we used a mean BA of $7.14 \times 10^5 \text{ cells mL}^{-1}$ and a mean BP of $0.031 \mu\text{g C L}^{-1}$

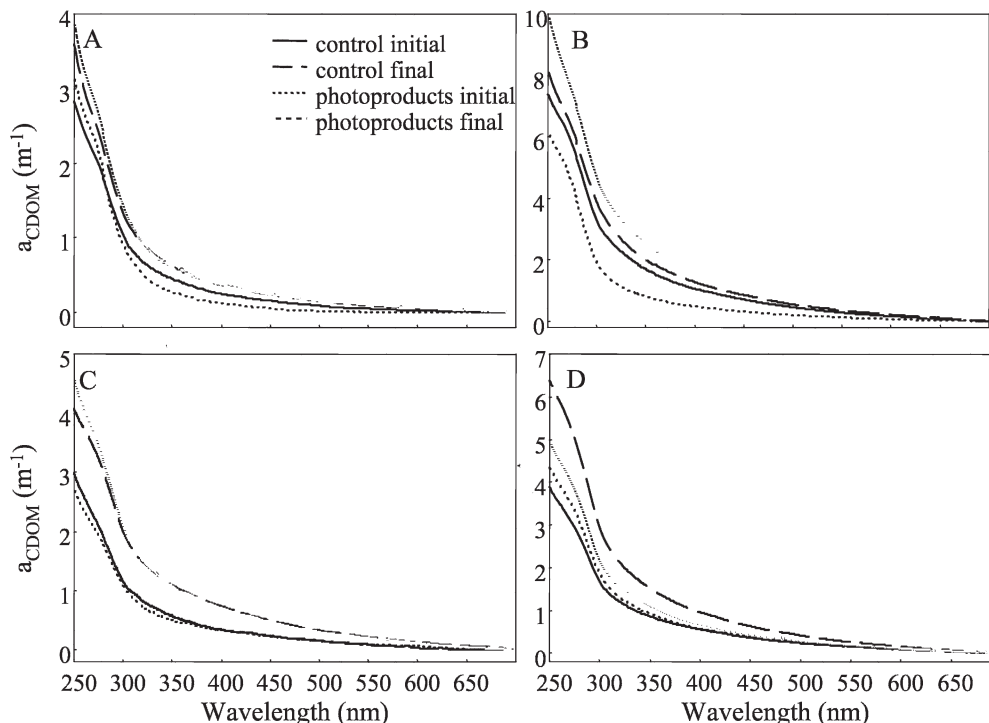


Fig. 1. CDOM absorption spectra from 250 to 700 nm at initial and final times of each treatment of the experiments performed with (A) Deception Island waters at 0 m, (B) Deception Island waters at 150 m, (C) Livingston Island waters at 0 m, and (D) Livingston Island waters at 50 m.

h^{-1} ; these values were based on sampling and experimentation in the same area determined during the cruise ICEPOS 2005 (Ortega-Retuerta et al. 2008).

We expressed experimental krill CDOM generation rates per organism and per liter as daily increases in $a_{325,443}$ ($\text{m}^{-1} \text{d}^{-1}$) subtracted by changes in CDOM per day in the controls without krill additions, and extrapolating to a density of one organism per liter correcting by the volume used in the incubations (0.7 and 2 liters). To extrapolate the experimental rates to field CDOM biogeneration by krill ($\text{m}^{-1} \text{d}^{-1}$), we used krill abundance data from the literature. We used an average krill density in spring–summer seasons in Antarctic waters between 1977 and 1996 of $77.78 \text{ individuals} \times 1000 \text{ m}^{-3}$ (Loeb et al. 1997), and a krill density within swarms of $1000 \text{ individuals m}^{-3}$ (Brierley and Watkins 2000).

We estimated CDOM duplication times attributable to bacterioplankton or to krill relating field data of $a_{325,443}$ in the Antarctic Peninsula area determined during the cruises ICEPOS 2004 and 2005 (mean $a_{325} = 0.34 \text{ m}^{-1}$, mean $a_{443} = 0.12 \text{ m}^{-1}$; Ortega-Retuerta et al. unpubl.) to the field CDOM generation rates derived from the experiments. We used the following equation:

$$\text{CDOM}_{\lambda} \text{ duplication time (d)} = \frac{\text{field CDOM}_{\lambda} (\text{m}^{-1})}{\text{field CDOM}_{\lambda} \text{ generation rates } (\text{m}^{-1} \text{d}^{-1})} \quad (4)$$

where λ is the reference wavelength (325 or 443 nm).

Results

The exposure of water to incident solar radiation to generate photoproducts for bacterial CDOM generation experiments yielded site-specific differences. Marked photobleaching of CDOM occurred in waters collected from Deception Island, irrespective of collection depth (Table 1, Fig. 1; 26–50% reduction in absorbance at 325 nm and 55–63% reduction in absorbance at 443 nm). The spectral slope $S_{275-295}$ increased in the treatment with photoproducts (Table 2). In contrast, little (4–12%) or no decrease in absorbance indicative of CDOM photobleaching was observed in waters collected from Livingston Island (Table 1; Fig. 1) and no relevant changes in the $S_{275-295}$ values in the treatment with photoproduct were detected (Table 2).

At the conclusion of the incubation periods, increases in a_{325} and a_{443} absorption coefficients and decreases in the values of $S_{275-295}$ were found in all bacterial regrowth cultures, irrespective of site, depth, or treatment imposed (Table 2). However, the magnitude of CDOM daily increase ($\Delta a_{325,443}$) was highly variable depending on the initial conditions of each incubation. For those experiments carried out with water from Deception Island, CDOM daily increases ($\Delta a_{325,443} \text{ m}^{-1} \text{d}^{-1}$) were significantly higher in the regrowth cultures with photoproducts than in those where photoproducts were absent (ANOVA, $p < 0.05$). The values of Δa_{325} ranged from 0.049 to $0.375 \text{ m}^{-1} \text{d}^{-1}$ and Δa_{443} ranged from 0.015 to $0.142 \text{ m}^{-1} \text{d}^{-1}$ (Table 2). The

Table 2. Spectral slopes from 275 to 295 ($S_{275-295}$) and the ratio of slopes (S_R) nm at the initial (t_0) and final time (t_f) of each treatment and daily CDOM increases at 325 and 443 nm ($m^{-1} d^{-1}$) and relative percentage with respect to initial absorption at 325 and 443 nm (d^{-1}) in all bacterial regrowth cultures (mean \pm standard error). No photo: treatments without photoproducts; photo: treatments with photoproducts.*

Location	Depth (m)	Treatment	$S_{275-295}$ t_0	$S_{275-295}$ t_f	S_R t_0	S_R t_f	Δa_{325} ($m^{-1} d^{-1}$)	Δa_{443} ($m^{-1} d^{-1}$)	% Δa_{325} (d^{-1})	% Δa_{443} (d^{-1})	ΔBA ($\times 10^5$ cell $mL^{-1} d^{-1}$)	ΔBP ($\mu g C$ $L^{-1} h^{-1}$) d^{-1}
Deception	0	no photo	0.0249	0.0231	1.91	2.19	0.056 \pm 0.011	0.023 \pm 0.001	8.9 \pm 1.7	13.8 \pm 0.8	3.69 \pm 0.04	0.139 \pm 0.016
		photo	0.0347	0.0242	1.96	2.50	0.099 \pm 0.003	0.048 \pm 0.002	21.6 \pm 0.7	76.9 \pm 2.6	0.87 \pm 0.08	0.214 \pm 0.017
		no photo	0.0216	0.0178	2.27	1.99	0.265 \pm 0.044	0.099 \pm 0.023	11.8 \pm 1.9	13.3 \pm 3.2	2.25 \pm 0.37	0.494 \pm 0.077
Livingston	0	no photo	0.0336	0.0186	3.29	2.07	0.375 \pm 0.014	0.142 \pm 0.007	33.4 \pm 1.3	43.3 \pm 2.0	1.06 \pm 0.06	0.424 \pm 0.020
		photo	0.0231	0.0192	2.22	2.46	0.126 \pm 0.048	0.056 \pm 0.018	16.2 \pm 6.2	23.1 \pm 7.3	0.34 \pm 0.12	0.064 \pm 0.055
		no photo	0.0227	0.0197	2.81	2.35	0.148 \pm 0.057	0.052 \pm 0.020	21.8 \pm 8.3	22.4 \pm 8.7	0.40 \pm 0.10	0.067 \pm 0.014
Livingston	50	no photo	0.0213	0.0200	2.45	2.33	0.172 \pm 0.019	0.057 \pm 0.005	15.2 \pm 1.7	14.8 \pm 1.3	0.32 \pm 0.05	0.052 \pm 0.009
		photo	0.0228	0.0213	2.21	2.18	0.049 \pm 0.010	0.015 \pm 0.001	4.0 \pm 0.8	3.8 \pm 0.3	0.73 \pm 0.20	0.061 \pm 0.001

* BA, bacterial abundance; BP, bacterial production.

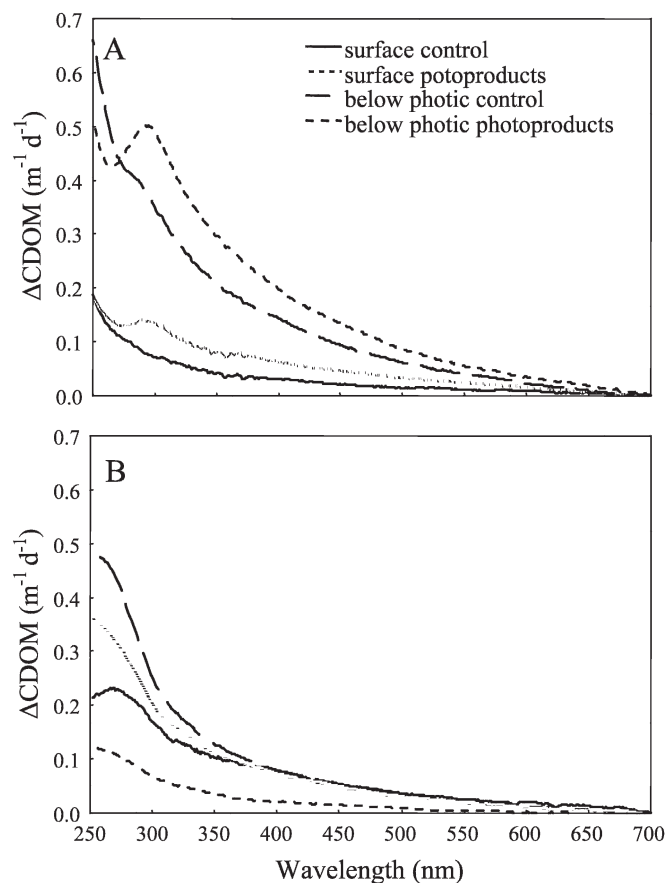


Fig. 2. Bacterially generated CDOM spectra from 250 to 700 nm (final – initial per day) in the different treatments using (A) Deception Island waters and (B) Livingston Island waters.

percentage of generated CDOM with respect to the initial absorption (% $\Delta a_{325,443}$) exhibited similar patterns.

In addition to the quantitative differences in CDOM generation observed in the different regrowth cultures, the spectral shape of bacterially generated CDOM also differed markedly. In the incubations carried out with water collected near Deception Island, where marked CDOM photobleaching was detected prior to the onset of the regrowth cultures (see Table 1; Fig. 1), CDOM spectra generated by bacteria showed distinctive peaks between 290 and 295 nm in the treatments with photoproducts (Fig. 2A). In comparison, the treatments without photoproducts exhibited the characteristic negative exponential shape (Fig. 2A). However, in the experiments performed using water from Livingston Island, where photobleaching was negligible, all CDOM spectra generated by bacteria were similar, with less-marked shoulders in the UVB region (Fig. 2B).

CDOM daily increases ($\Delta a_{325,443}$) attributed to bacteria in the incubations were significant ($p < 0.05$) and positively related to daily increases in BP ($r^2 = 0.59$ and $r^2 = 0.62$, respectively). Likewise, daily CDOM increases were related to average BP in the incubations (Fig. 3), but not to BA. The slopes of the regression lines passing through the origin, not significantly different from the regression lines with the intercept, were used as estimates of bacterial

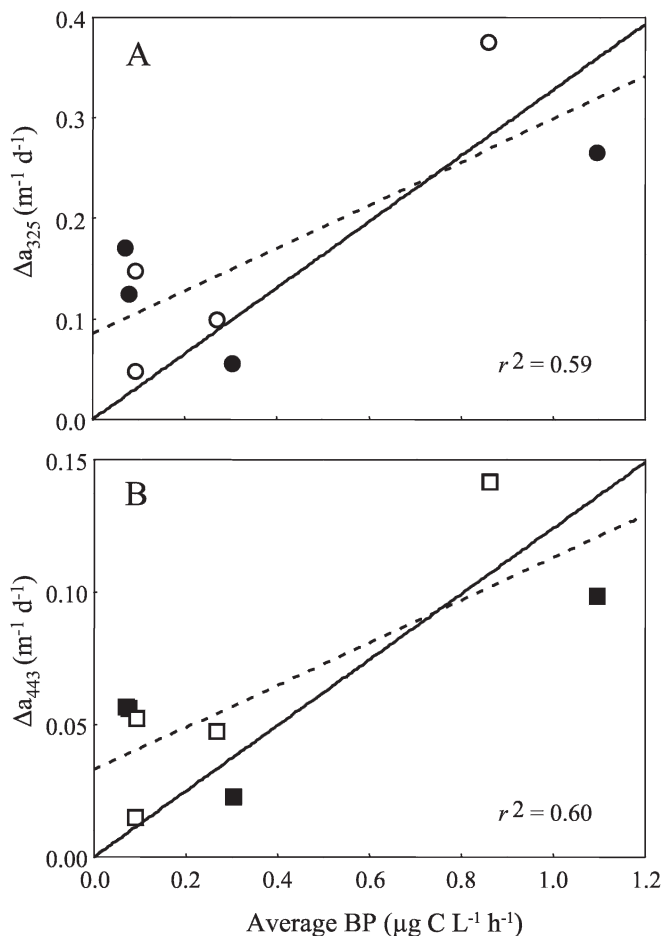


Fig. 3. Relationships between (A) Δa_{325} or (B) Δa_{443} in all regrowth experiments and average BP. Open symbols: treatments with photoproducts. Filled symbols: treatments without photoproducts. Solid lines represent the regression lines passing through the origin, and dashed lines represent the regression lines with the intercept. In no case are the two equations significantly different ($p > 0.05$). The slopes of the solid lines represent the experimental bacterial CDOM generation rates ($\text{m}^{-1} \text{d}^{-1}$ per $\mu\text{g C L}^{-1} \text{h}^{-1}$; see Table 3).

CDOM generation rates without reference to the CDOM baseline (intercept) and, hence, extrapolable to other ocean areas (Table 3). An extrapolation of these experimental rates ($\Delta a_{325,443}$ per unit of BP) to field BP average values yielded estimates of CDOM generation rates of $10.2 \times$

Table 3. Bacteria CDOM generation rates of absorption at 325 nm and 443 nm obtained experimentally and calculated from BP ($\text{m}^{-1} \text{d}^{-1}$ per $\mu\text{g C L}^{-1} \text{h}^{-1}$), field bacterial CDOM generation rates at 325 and 443 nm ($\text{m}^{-1} \text{d}^{-1}$) estimated for field conditions in the Southern Ocean, and CDOM duplication times (d).

	Reference wavelength (nm)	
	325	443
Experimental a_λ generation rate ($\text{m}^{-1} \text{d}^{-1}$ per $\mu\text{g C L}^{-1} \text{h}^{-1}$)	0.3275 ± 0.07	0.1241 ± 0.07
Field Δa_λ ($\times 10^{-3} \text{m}^{-1} \text{d}^{-1}$)	10.2	3.8
Field a_λ duplication time (d)	33	31

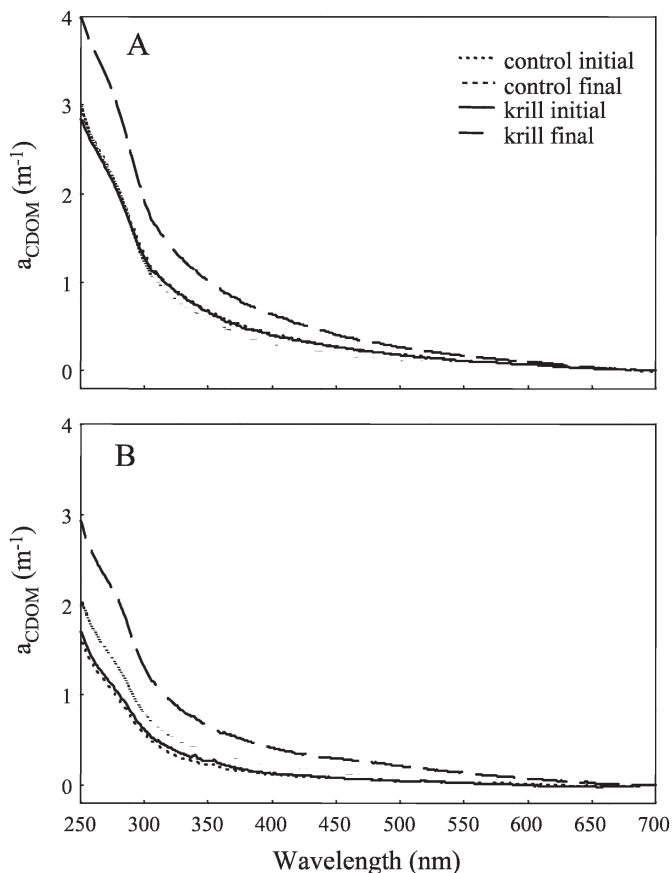


Fig. 4. CDOM absorption spectra from 250 to 700 nm at initial and final times of krill experiments (A) 9 and (B) 13 with their respective controls without krill additions.

$10^{-3} \text{m}^{-1} \text{d}^{-1}$ at 325 nm and $3.8 \times 10^{-3} \text{m}^{-1} \text{d}^{-1}$ at 443 nm (Table 3). These CDOM generation rates suggest CDOM duplication times of 31–33 d (Table 3).

Significant ($p < 0.05$) increases in CDOM (as indicated by changes in absorbance at 325 and 443 nm) were detected in most daily incubations (12 of 15) with adult krill when compared to changes in control treatments, where no changes or decreases in CDOM were observed (Fig. 4). In those incubations with krill where an increase in CDOM was observed, Δa_{325} ranged from 0.132 to $1.535 \text{m}^{-1} \text{d}^{-1}$ and Δa_{443} ranged from 0.043 to $0.524 \text{m}^{-1} \text{d}^{-1}$ (Table 4). We detected increases at 325 nm in all hourly incubations (Nos. 16–20), with Δa_{325} ranging from 0.525 to $1.416 \text{m}^{-1} \text{d}^{-1}$. However, increases at 443 nm were detected in only three of five hourly incubations (Table 4). The shapes of the CDOM spectra differed markedly between daily and hourly experiments. CDOM generated by krill in daily incubations tended to exhibit higher absorption coefficients at shorter wavelengths ($< 300 \text{nm}$), with a shoulder at 290–295 nm (Fig. 5A). By contrast, CDOM generated by krill in hourly experiments consistently exhibited two distinct peaks, at 270–280 nm and at 340–345 nm (Fig. 5B). These peculiar spectral shapes prevented the calculations of $S_{275-295}$ at the end of incubations, and only the initial values are reported in Table 4.

Table 4. Initial values of Chl *a*, dissolved organic carbon (DOC) concentration, a_{325} , the spectral slope $S_{275-295}$, the ratio of slopes S_R , and the daily CDOM increases ($m^{-1} d^{-1}$) and percentages of CDOM increase (d^{-1}) at 325 and 443 nm in all krill incubations (Inc No.).*

Inc No.	Inc type	Inc time (h)	Chl <i>a</i> ($\mu g L^{-1}$)	DOC ($\mu mol L^{-1}$)	a_{325} (m^{-1})	$S_{275-295}$ t_0	S_R t_0	Δa_{325} ($m^{-1} L^{-1} d^{-1}$)	Δa_{443} ($m^{-1} L^{-1} d^{-1}$)	% Δa_{325} (d^{-1})	% Δa_{443} (d^{-1})
1	daily	21	10.4	72	1.101	0.013	1.35	-1.348	-0.403	-119	-107
2	daily	21	10.4	72	1.101	0.013	1.35	-1.299	-0.432	-95	-92
3	daily	21	10.4	72	1.101	0.013	1.35	-1.114	-0.385	-138	-130
4	daily	19	9.7	176	1.453	0.018	2.07	0.651	0.229	45	44
5	daily	19	9.7	176	1.453	0.018	2.07	0.360	0.115	25	22
6	daily	19	9.7	176	1.453	0.018	2.07	0.192	0.043	13	8
7	daily	19	9.7	176	1.453	0.018	2.07	0.540	0.150	37	29
8	daily	12	5.65	70	0.901	0.020	2.02	0.646	0.315	64	101
9	daily	12	5.65	70	0.901	0.020	2.02	1.059	0.453	119	161
10	daily	12	5.65	70	0.901	0.020	2.02	0.132	0.122	14	42
11	daily	13	2.55	68	0.326	0.024	1.92	0.496	0.084	137	60
12	daily	13	2.55	68	0.326	0.024	1.92	1.535	0.524	509	785
13	daily	13	2.55	68	0.326	0.024	1.92	0.593	0.264	157	310
14	daily	13	2.55	68	0.326	0.024	1.92	0.302	0.132	71	115
15	daily	13	2.55	68	0.326	0.024	1.92	0.655	0.185	154	130
16	hourly	4	0.12	na	0.198	0.023	1.15	1.416	-0.028	715	-60
17	hourly	3	0.45	na	0.196	0.032	1.12	0.525	0.046	268	95
18	hourly	4	1.12	na	0.385	0.026	2.48	0.864	0.193	225	165
19	hourly	4	0.64	na	0.219	0.030	2.04	1.099	0.014	502	27
20	hourly	4	7.69	na	0.573	0.023	1.15	1.092	-0.276	190	-316

* na, not analyzed.

To assess the potential effect of bacterial growth on CDOM generation in the krill incubations, and then to correct the values of CDOM generated and attributed exclusively to krill, we monitored BP and BA in parallel. In daily experiments, BP showed hourly increases of $0.0086 \mu g C L^{-1} h^{-1}$ and BA showed hourly increases of $656 cells mL^{-1}$. Thus, even correcting for bacterial contributions due to BP, 12 of the 15 daily incubations showed CDOM daily increases at a_{325} and a_{443} . Bacterial growth was not detected in hourly experiments.

Biogeneration rates by krill, after corrections for potential CDOM bacterial contributions and extrapolated to a density of one organism per liter, averaged (daily and hourly experiments) $0.715 m^{-1} d^{-1}$ for a_{325} and $0.151 m^{-1} d^{-1}$ for a_{443} (Table 5). Extrapolating krill CDOM generation rates to field data, we estimated field Δa_{325} of $0.055 \times 10^{-3} m^{-1} d^{-1}$ and field Δa_{443} of $0.012 \times 10^{-3} m^{-1} d^{-1}$, considering average krill densities around the Antarctic Peninsula of 77.8 individuals in $1000 m^3$ (Loeb et al. 1997) (Table 5). The application of these average CDOM generation values to the study area would yield a CDOM duplication time of years. Considering 1000 organisms per cubic meter as a representative density of krill swarms (Brierley and Watkins 2000), field CDOM generation would be analogous to the experimentally determined krill CDOM generation rates ($\Delta a_{325,443}$ per org L^{-1}), and would imply CDOM duplication times from 0.48 to 0.80 d (Table 5).

Discussion

Bacterial generation of CDOM was evident in all regrowth cultures and confirms the potential role of bacteria as a CDOM source in the Southern Ocean. Field

work based on CDOM seasonal dynamics (Nelson et al. 1998), fluorescent DOM dynamics and distribution (Yamashita et al. 2007; Yamashita and Tanoue 2008), and changes in BA within phytoplankton cultures or mesocosms (Rochelle-Newall and Fisher 2002) had previously inferred this linkage. In fact, bacterial CDOM generation has been experimentally confirmed (Kramer and Herndl 2004; Nelson et al. 2004; Biers et al. 2007). However, quantitative bacterial CDOM generation rates are hardly comparable among these published studies, because different analytical approaches were employed (absorbance vs. fluorescence, different reference wavelengths). The percentages of CDOM increase (d^{-1}) reported herein are consistent, however, with values reported by Nelson et al. (2004) for BP rates (from 12 to $120 d^{-1}$) during the exponential growth phase.

The consistent CDOM generation by bacteria and net decrease in the $S_{275-295}$ values in all treatments of the different regrowth cultures (Table 2) indicate that CDOM bacterial generation could be associated with an increase of DOM molecular weight, as has been previously reported (Helms et al. 2008). The magnitude and spectral quality of generated CDOM was, however, different depending on the presence or absence of photoproducts as a substrate. In those treatments where marked photobleaching was evident (incubations carried out with water collected near Deception Island), CDOM generation was greater, suggesting that photoaltered CDOM is more susceptible to further bacterial processing. In addition, bacterially generated CDOM from photoaltered DOM exhibited a distinct spectral shape, with maximum absorbance at 290–295 nm, providing additional insight into the nature of the transformations. This particular spectral shape might be

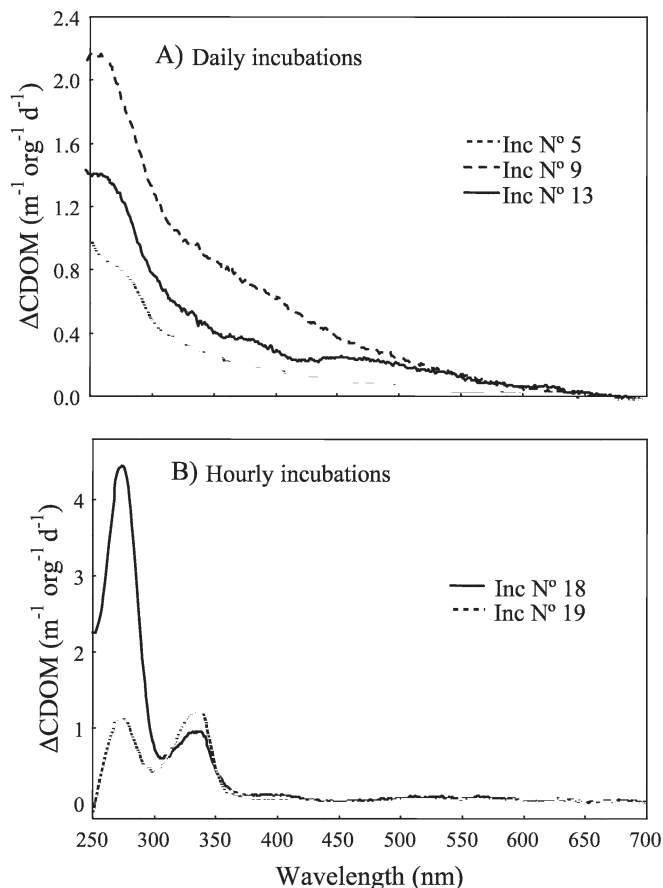


Fig. 5. Krill-generated CDOM spectra (daily CDOM increases per organism and day, normalized by daily changes in the control treatments) in three representative krill daily incubations (inc) (numbers 5, 9, and 13, upper panel) and two representative krill hourly incubations (numbers 18 and 19, bottom panels; see also Table 4).

attributed to the selective growth of specific bacterial populations. In this sense, the percentage of the assemblage that would have passed through the GF/F filters, and, hence, been subjected to irradiation, although minor (12–15%), could be responsible of some of the generated CDOM. On the one hand, the spectral shape of bacterially generated CDOM could be related to unique properties of the initial DOM. Indeed, Deception Island is a semi-

Table 5. Experimental average of generation rates by krill in the incubations ($\text{m}^{-1} \text{d}^{-1}$ per organism L^{-1}), estimated field CDOM generation rates at 325 and 443 nm ($\text{m}^{-1} \text{d}^{-1}$), and field CDOM duplication times within swarms (d). Krill CDOM generation rates are corrected by potential bacterial contributions using bacterial production.

	Reference wavelength (nm)	
	325	443
Krill a_z generation rate	0.715 ± 0.099	0.151 ± 0.045
Field Δa_z ($\times 10^{-3} \text{m}^{-1} \text{d}^{-1}$)	0.055	0.012
Field a_z duplication time (d) within swarms	0.48	0.80

enclosed bay with high Chl *a* levels (see Table 1) where DOM is likely to be of recent algal origin and, thus, likely more photo- and bioreactive. On the other hand, the lack of significant CDOM photobleaching observed in waters from Livingston Island is possibly attributable to the more refractory nature of DOM or to the lower cumulative sunlight dose received in the photoproduct treatments of the Livingston Island experiments. There was a similar response in bacterially generated CDOM generation in all treatments, irrespective of the presence or absence of photoproducts, showing more typical negative exponential absorption spectra.

In this work, we demonstrate a direct link between bacterial activity and CDOM biogeneration, irrespective of initial CDOM, mineral nutrient concentration, or the presence or absence of photoproducts, explaining about 60% of the variance in ΔCDOM by BP (Fig. 3), and we provide equations potentially applicable to other ocean areas. This link confirms the predominant role of bacterial DOM processing over other potential processes affecting CDOM generation, such as viral lysis or cell death. This key role of bacterial activity has been also suggested by Yamashita and Tanoue (2008), who found a tight relationship between apparent oxygen utilization and fluorescent DOM in the deep ocean.

Extrapolation of our rates to field conditions predicts a CDOM duplication time of 31–33 d, considering average BP values in the Antarctic Peninsula area during austral summer (Ortega-Retuerta et al. 2008). However, in areas where high BP values were reported (e.g., in the western Weddell Sea during ice-free periods, where BP can reach $0.111 \mu\text{g C h}^{-1} \text{L}^{-1}$), CDOM duplication times of about 10 d are possible. Thus, we have demonstrated that bacteria can generate significant amounts of CDOM on a short (i.e., less than a week) timescale. The effect of bacteria on CDOM dynamics will depend on the persistence of the bacterially generated CDOM in the environment, which can range from labile material, consumed or degraded in a few days (Nelson et al. 2004; Biers et al. 2007), to refractory material (Ogawa et al. 2001), a feature that appears to be dependent on nitrogen availability (Biers et al. 2007). The study of the persistence of the CDOM generated by bacteria into the water column has relevance for ocean DOC storage and deserves further investigation in the context of global carbon cycling.

Our results also provide the first evidence for the potential of Antarctic krill, *E. superba*, to contribute to the CDOM pool in the Southern Ocean. Previous studies have reported the release of CDOM and fluorescent DOM by different zooplankton species (Steinberg et al. 2004; Urban-Rich et al. 2006) indicating that these organisms could be responsible for unique CDOM and fluorescent DOM signatures. In this study, we observed two different spectral shapes for krill-generated CDOM, depending on incubation time. Considering hourly incubations (less than 4 h), CDOM spectra showed two distinct peaks at ≈ 290 and 340 nm (see Fig. 5B). By contrast, in daily incubations we did not observe the peak at the 330–340-nm region, and a shoulder at 290 nm was visible but less evident. This difference in the spectral shape between the hourly and

daily incubations could be related to the release of specific compounds such as urea (Glibert 1998) that may disappear quickly. This finding is consistent with a previous report of CDOM excretion by euphausiids (Steinberg et al. 2004). In the daily incubations, higher initial CDOM values, along with a greater bacterial influence (generating CDOM at shorter wavelengths) could have masked CDOM attributed exclusively to krill release.

All krill incubations showed CDOM production except for one complete set of incubations (daily experiments 1–3; see Table 4). This result suggests that CDOM production by Antarctic krill is likely dependent on other factors, such as ambient conditions, the nutritional status of the organisms, or short-term cycling of CDOM during the incubation. These factors merit further attention because only single measurements were made in our study. Indeed, in the aforementioned set of incubations, abnormally high background levels of CDOM at time 0 were observed (data not shown), which could have masked the krill contribution.

The relevance of estimating the potential contributions of Antarctic krill to CDOM dynamics is underscored by their status as a keystone species in the Southern Ocean; krill are both important grazers (Ross et al. 1998) and preferential prey for most higher-order consumers, including seals, penguins, whales, and seabirds (Croxall et al. 1999), and they affect biogeochemical cycling as well (Tovar-Sánchez et al. 2007). Accordingly, CDOM duplication times attributable to krill would be generally an order of magnitude longer than CDOM duplication times attributable to bacteria when considering average seasonal krill densities in waters around the Antarctic Peninsula (Loeb et al. 1997). Whereas this could suggest a minor role of krill on CDOM dynamics, these organisms can form large swarms with hundreds to thousands of organisms per cubic meter (Brierley and Watkins 2000), where CDOM duplication times would be shorter than a day (Table 5). Therefore, an intense and unique CDOM signal is expected in association with krill swarms or areas recently occupied by krill swarms. Because krill activity releases large amounts of labile organic carbon, ammonium, and other limiting elements such as phosphate or iron (Quetin et al. 1994; Tovar-Sánchez et al. 2007), krill activity could greatly stimulate bacterioplankton growth, fueling further bacterial CDOM generation.

Overall, our findings highlight the potential significance of bacteria and Antarctic krill swarms in the generation of CDOM in the Southern Ocean. CDOM duplication times from days (considering CDOM in krill swarms) to months (considering bacterial activity) or years (considering average krill densities) in the area underscore the dynamic nature of CDOM. Additional studies will be required to assess the persistence of biologically generated CDOM in order to evaluate the realized effect of bacteria and krill on the spatial and temporal dynamics of CDOM and DOC cycling in the Southern Ocean.

Acknowledgments

We extend our thanks to R. Ross and L. Quetin for providing the krill specimens used in our 2004 experiments and to Miquel

Alcaraz for assistance to capture those used in our 2009 experiments. We thank the Marine Technology Unit, particularly J. Linás del Torrent, R. Ametller, and M. Pastor, for logistic assistance, and R. Martínez and P. Echeveste for Chl *a* and nitrogen analyses. We also acknowledge the associate editor, Stephen P. Opsahl, and three anonymous reviewers for their helpful comments on a previous version of this MS. This work was funded by the Spanish Ministry of Science and Innovation through projects REN2002-04165-CO3-02 and POL2006-00550/CTM to C.M.D. and CGL2005-00076 to I.R., and the United States National Science Foundation (NSF-OPP award 0336469) to T.K.F. E.O.-R. was supported by a fellowship of the Spanish Ministry of Science and Education.

References

- BIERS, E. J., R. G. ZEPP, AND M. A. MORAN. 2007. The role of nitrogen in chromophoric and fluorescent dissolved organic matter formation. *Mar. Chem.* **103**: 46–60.
- BRICAUD, A., A. MOREL, AND L. PRIEUR. 1981. Absorption by dissolved organic-matter of the sea (yellow substance) in the UV and visible domains. *Limnol. Oceanogr.* **26**: 43–53.
- BRIERLEY, A. S., AND J. L. WATKINS. 2000. Effects of sea ice cover on the swarming behaviour of Antarctic krill, *Euphausia superba*. *Can. J. Fish. Aquat. Sci.* **57**: 24–30.
- COBLE, P. G. 2007. Marine optical biogeochemistry: The chemistry of ocean color. *Chem. Rev.* **107**: 402–418.
- CROXALL, J. P., K. REID, AND P. A. PRINCE. 1999. Diet, provisioning and productivity responses of marine predators to differences in availability of Antarctic krill. *Mar. Ecol. Prog. Ser.* **177**: 115–131.
- GLIBERT, P. M. 1998. Interactions of top-down and bottom-up control in planktonic nitrogen cycling. *Hydrobiologia* **363**: 1–12.
- HELMS, J. R., A. STUBBINS, J. D. RITCHIE, E. C. MINOR, D. J. KIEBER, AND K. MOPPER. 2008. Absorption spectral slopes and slope ratios as indicators of molecular weight, source, and photobleaching of chromophoric dissolved organic matter. *Limnol. Oceanogr.* **53**: 955–969.
- KAWASAKI, N., AND R. BENNER. 2006. Bacterial release of dissolved organic matter during cell growth and decline: Molecular origin and composition. *Limnol. Oceanogr.* **51**: 2170–2180.
- KIEBER, R. J., L. H. HYDRO, AND P. J. SEATON. 1997. Photo-oxidation of triglycerides and fatty acids in seawater: Implication toward the formation of marine humic substances. *Limnol. Oceanogr.* **42**: 1454–1462.
- KRAMER, G. D., AND G. J. HERNDL. 2004. Photo- and bioreactivity of chromophoric dissolved organic matter produced by marine bacterioplankton. *Aquat. Microb. Ecol.* **36**: 239–246.
- LOEB, V., V. SIEGEL, O. HOLM-HANSEN, R. HEWITT, W. FRASERK, W. TRIVELPIECK, AND S. TRIVELPIECK. 1997. Effects of sea-ice extent and krill or salp dominance on the Antarctic food web. *Nature* **387**: 897–900.
- MOPPER, K., X. L. ZHOU, R. J. KIEBER, D. J. KIEBER, R. J. SIKORSKI, AND R. D. JONES. 1991. Photochemical degradation of dissolved organic carbon and its impact on the oceanic carbon cycle. *Nature* **353**: 60–62.
- MORAN, M. A., AND R. G. ZEPP. 1997. Role of photoreactions in the formation of biologically labile compounds from dissolved organic matter. *Limnol. Oceanogr.* **42**: 1307–1316.
- NELSON, N. B., C. A. CARLSON, AND D. K. STEINBERG. 2004. Production of chromophoric dissolved organic matter by Sargasso Sea microbes. *Mar. Chem.* **89**: 273–287.
- , AND D. A. SIEGEL. 2002. Chromophoric DOM in the open ocean. *In* D. A. Hansell and C. A. Carlson [eds.], *Biogeochemistry of marine dissolved organic matter*. Academic.

- , ———, AND A. F. MICHAELS. 1998. Seasonal dynamics of colored dissolved material in the Sargasso Sea. *Deep-Sea Res. I* **45**: 931–957.
- NICOL, S. 2006. Krill, currents, and sea ice: *Euphausia superba* and its changing environment. *Bioscience* **56**: 111–120.
- OGAWA, H., Y. AMAGAI, I. KOIKE, K. KAISER, AND R. BENNER. 2001. Production of refractory dissolved organic matter by bacteria. *Science* **292**: 917–920.
- ORTEGA-RETUERTA, E., I. RECHE, E. PULIDO-VILLENA, S. AGUSTI, AND C. M. DUARTE. 2008. Exploring the relationship between active bacterioplankton and phytoplankton in the Southern Ocean. *Aquat. Microb. Ecol.* **52**: 99–106.
- PARSONS, T. R., Y. MAITA, AND C. M. LALLI. 1984. A manual of chemical and biological methods for sea water analysis. Pergamon.
- PORTER, K. G., AND Y. S. FEIG. 1980. The use of DAPI for identifying and counting aquatic microflora. *Limnol. Oceanogr.* **25**: 943–948.
- QUETIN, L. B., R. M. ROSS, AND A. CLARKE. 1994. Krill energetics: Seasonal and environmental aspects of the physiology of *Euphausia superba*, p. 161–184. In S. El-Sayed [ed.], *Southern ocean ecology: The BIOMASS perspective*. Cambridge Univ. Press.
- RECHE, I., E. PULIDO-VILLENA, J. M. CONDE-PORCUNA, AND P. CARRILLO. 2001. Photoreactivity of dissolved organic matter from high-mountain lakes of Sierra Nevada, Spain. *Arct. Antarct. Alp. Res.* **33**: 426–434.
- ROCHELLE-NEWALL, E. J., AND T. R. FISHER. 2002. Production of chromophoric dissolved organic matter fluorescence in marine and estuarine environments: An investigation into the role of phytoplankton. *Mar. Chem.* **77**: 7–21.
- ROSS, R. M., L. B. QUETIN, AND K. L. HABERMAN. 1998. Interannual and seasonal variability in short-term grazing impact of *Euphausia superba* in nearshore and offshore waters west of the Antarctic Peninsula. *J. Mar. Syst.* **17**: 261–273.
- SIEGEL, D. A., S. MARITORENA, N. B. NELSON, AND M. J. BEHRENFELD. 2005. Independence and interdependencies among global ocean color properties: Reassessing the bio-optical assumption. *J. Geophys. Res. Oceans* **110**: C07011, doi: 10.1029/2004JC002527.
- , ———, ———, D. A. HANSELL, AND M. LORENZI-KAYSER. 2002. Global distribution and dynamics of colored dissolved and detrital organic materials. *J. Geophys. Res. Oceans* **107**: 3228, doi: 10.1029/2001JC000965.
- SIMON, M., AND F. AZAM. 1989. Protein-content and protein-synthesis rates of planktonic marine-bacteria. *Mar. Ecol. Prog. Ser.* **51**: 201–213.
- SMITH, D. C., AND F. AZAM. 1992. A simple economical method for measuring bacterial protein synthesis rates in seawater using ³H-leucine. *Mar. Microb. Food Webs* **6**: 107–114.
- STEINBERG, D. K., N. B. NELSON, C. A. CARLSON, AND A. C. PRUSAK. 2004. Production of chromophoric dissolved organic matter (CDOM) in the open ocean by zooplankton and the colonial cyanobacterium *Trichodesmium* spp. *Mar. Ecol. Progr. Ser.* **267**: 45–56.
- TOVAR-SANCHEZ, A., C. M. DUARTE, S. HERNÁNDEZ-LEÓN, AND S. A. SAÑUDO-WILHELMY. 2007. Krill as a central node for iron cycling in the Southern Ocean. *Geophys. Res. Lett.* **34**: L11601, doi: 10.1029/2006GL029096.
- TRANVIK, L. J. 1993. Microbial transformations of labile organic matter into humic-like matter in seawater. *FEMS Microbiol. Ecol.* **12**: 177–183.
- URBAN-RICH, J., J. T. MCCARTY, D. FERNANDEZ, AND J. L. ACUÑA. 2006. Larvaceans and copepods excrete fluorescent dissolved organic matter (FDOM). *J. Exp. Mar. Biol. Ecol.* **332**: 96–105.
- YAMASHITA, Y., AND E. TANOUE. 2008. Production of bio-refractory fluorescent dissolved organic matter in the ocean interior. *Nat. Geosci.* **1**: 579–582.
- , A. TSUKASAKI, T. NISHIDA, AND E. TANOUE. 2007. Vertical and horizontal distribution of fluorescent dissolved organic matter in the Southern Ocean. *Mar. Chem.* **106**: 498–509.

Associate editor: Stephen P. Opsahl

Received: 20 June 2008

Accepted: 06 May 2009

Amended: 29 June 2009